Published online January 23, 2004

Nucleic Acids Research, 2004, Vol. 32, No. 2 ***e18***
DOI: 10.1093/nar/gnh013

Rapid detection of single nucleotide polymorphisms associated with spinal muscular atrophy by use of a reusable fibre-optic biosensor

James H. Watterson, Sandeep Raha, Christopher C. Kotoris, Christopher C. Wust, Farhad Gharabaghi, Sarah C. Jantzi, Nicole K. Haynes, Nathalie H. Gendron[1], Ulrich J. Krull, Alex E. Mackenzie[1] and Paul A. E. Piunno*

Chemical Sensors Group, University of Toronto at Mississauga, 3359 Mississauga Road North, Mississauga, Ontario, Canada L5L 1C6 and [1]Children's Hospital of Eastern Ontario Research Institute, Molecular Genetics Laboratory, 401 Smyth Road, Ottawa, Ontario, Canada K1H 8L1

Received September 30, 2003; Revised November 6, 2003; Accepted December 2, 2003

ABSTRACT

Rapid (<2 min) and quantitative genotyping for single nucleotide polymorphisms (SNPs) associated with spinal muscular atrophy was done using a reusable (approximately 80 cycles of application) fibre-optic biosensor over a clinically relevant range (0–4 gene copies). Sensors were functionalized with oligonucleotide probes immobilized at high density (~7 pmol/cm^2) to impart enhanced selectivity for SNP discrimination and used in a total internal reflection fluorescence detection motif to detect 202 bp PCR amplicons from patient samples. Real-time detection may be done over a range of ionic strength conditions (0.1–1.0 M) without stringency rinsing to remove non-selectively bound materials and without loss of selectivity, permitting a means for facile sample preparation. By using the time-derivative of fluorescence intensity as the analytical parameter, linearity of response may be maintained while allowing for significant reductions in analysis time (10–100-fold), permitting for the completion of measurements in under 1 min.

INTRODUCTION

The goal of this research is to investigate the design and immobilization of nucleic acid probes for development of reusable sensors that display rapid, selective, sensitive and quantitative response to a particular target in a complex matrix. Current methodologies for single nucleotide polymorphism (SNP) screening often require amplification, followed by time-consuming enzymatic manipulation (e.g. digestion or extension) and separation of the resultant products. New sensor and microarray technologies attempt to simplify SNP analysis, but most require many hours for hybridization and data analysis (1). The sensing methodology that is described here demonstrates significant improvements over established and emerging nucleic acid diagnostic technologies (2–4) in terms of time of analysis and reusability, while maintaining high selectivity so that quantitative SNP analysis may be possible. This system represents an easily scalable device for the quantitative estimation of relative SNP quantity without the need for stringency washing following equilibration. Sensors have been observed to function reliably over 80 cycles of application, with all sensors used in this work demonstrating these features for more than 10 cycles of application without loss of sensitivity.

Current protocols for genotyping and expression analysis involve amplification or solid-phase hybridization (5–7). More recently, advancements in real-time PCR methods (8) permit simultaneous amplification and quantification. Unfortunately, non-specific amplification may not always be discernable and quantitative determinations based on measurement of amplification products can be challenging due to secondary-structure and sample matrix effects (9,10). Although a more time-consuming method, post-amplification thermal denaturation analysis may improve selectivity of detection, but is most effective when there are significant differences between the product and target (11). Microarrays permit large-scale screening of nucleic acid targets via monitoring interfacial hybridization. However, microarray data require significant bioinformatic processing (1) and microarrays often cannot be reused as a result of the chemistry used for nucleic acid immobilization. Difficulties associated with control of homogeneity of probe distribution, probe density and probe sequence length (when using *in situ* synthesis) can result in variations in the thermal denaturation temperature (T_m) of the interfacial hybrids from spot to spot or within a given array element. Regions on the substrate exhibiting variations in selectivity, kinetics and dynamic range of response at any given temperature and composition of the sample solution can therefore occur. These phenomena may contribute to a reduction in the selectivity of hybridization, as evidenced by broadening of the thermal denaturation transition with respect to temperature (12). Overall, this implies that significant redundancy in probe sequence is required to improve signal-to-noise ratios to affect quantitative measurements (13). An

*To whom correspondence should be addressed. Tel: +1 905 828 5453; Fax: +1 905 828 5425; Email: ppiunno@utm.utoronto.ca

 © Oxford University Press 2004; all rights reserved

alternative to such an approach is the use of highly controlled covalent immobilization methodologies in a sensor format to facilitate a reusable, quantitative technology where selectivity and kinetics may be more closely controlled. Furthermore, advantages in terms of enhancement of selectivity may be realized through such control of the interfacial nucleic acid film chemistry.

The fibre-optic nucleic acid biosensor is based upon the use of probe oligonucleotides that are covalently immobilized to the surface of fused silica optical fibres and operates using a total internal reflection fluorescence (TIRF) detection modality. Fluorescence from Cy5 labels associated with the target nucleic acids (oligonucleotides and larger PCR amplicons) hybridized to immobilized capture probes on the sensor surface was excited and collected from the fibre waveguide in an intrinsic mode optical sensor configuration (14). This detection modality provides for quantitative and selective detection of fluorophores situated at the sensor surface. There are minimal contributions from fluorophores in bulk solution, other than those interrogated beyond the unblocked distal terminus of the fibres.

The clinical utility of this sensor technology was demonstrated by evaluation of genetic markers associated with spinal muscular atrophy (SMA). This childhood neuromuscular disease is characterized by the loss of alpha-motor neurons leading to symmetrical wasting of the voluntary muscles (15). Mutations in the *SMN1* gene, leading to pathologic reductions in survival of motor neuron (SMN) protein levels is the primary cause of SMA. Deletions or mutations in *SMN1* alone (16) cannot explain the broad spectrum of severity found in SMA patients. The answer is found in the presence of a second gene, a result of an *SMN1* gene duplication, known as *SMN2* which is found in all SMA patients. Although *SMN1* and *SMN2* mRNAs differ by 5 nt substitutions near the 3′-termini (none of which result in coding changes), *SMN2* makes a truncated, less stable, product (17,18). The C→T mutation in *SMN2* exon 7 has been shown to be the primary cause for this defective splicing (18). In broad terms, the absence of *SMN1* is diagnostic of SMA, haploinsufficiency of *SMN1* reflects SMA carrier status and *SMN2* copy number will give a rough indication of anticipated clinical severity (19,20). We have thus configured a suite of sensors to estimate both *SMN1* and *SMN2* copy number consisting of 19 bp oligomers derived from the intron 6/exon 7 splice-site between *SMN1* and *SMN2* genes in addition to a negative control sensor (Table 1).

Table 1. Oligonucleotide sequences used as immobilized probes and labeled targets in thermal denaturation and SNP analysis experiments

Oligonucleotide	Sequence
SMN1 (immobilized probe)	5′-A TTT TGT CT***G*** AAA CCC TGT-3′
*SMN1*A (Cy5-labeled target)	5′-Cy5-ACA GGG TTT ***C***AG ACA AAA T-3′
SMN2 (immobilized probe)	5′-A TTT TGT CT***A*** AAA CCC TGT-3′
*SMN2*A (Cy5-labeled target)	5′-Cy5-ACA GGG TTT ***T***AG ACA AAA T-3′
uidA (reference sensor) (immobilized probe)	5′-AGT CTT ACT TCC ATG ATT TCT TTA ACT ATG-3′

SNP sites are shown in bold italics.

MATERIALS AND METHODS

Sensor production

Oligonucleotides probes that were 19 nt in length (Table 1) and selective for either *SMN1* or *SMN2* gene fragments were covalently immobilized to the surface of fused silica optical fibre segments (48 mm length × 0.400 mm diameter; Innova Quartz, AZ) by automated oligonucleotide synthesis (21). The analysis of immobilized oligonucleotides for density and film homogeneity in terms of the fidelity of the assembled oligonucleotides was done by anion-exchange HPLC (22). The sensors were designed so that the SNP site would be situated in the center of the probe-target hybrid. Disruption of the base pairing in this position was expected to cause the greatest reduction of hybrid stability.

Oligonucleotides for use as targets in thermal denaturation experiments and as primers for PCR amplification of patient sample DNA were synthesized using an ABI 394 synthesizer as described elsewhere (21). Where necessary, oligonucleotides were labeled on the 5′-terminus by means of automated synthesis methods using Cy5 phosphoramidites (Amersham Pharmacia, Mississauga, ON, Canada).

Amplification of *SMN1* and *SMN2* gene fragments from patient DNA

SMA and control fibroblasts cell lines were purchased from the Coriell Institute (New Jersey, USA). Genomic DNA was isolated and a 202 bp PCR product was amplified from the *SMN1* and *SMN2* genes using the following primers, 5′-(Cy5)CCTTTTATTTTCCTTACA-GGGTTT-3′ (*SMN202*-F) and 5′-TGATTGTTTTAC-ATTAACCTTTCAA-3′ (*SMN202*-R). Amplifications were done asymmetrically using an annealing temperature of 53°C for 35 cycles and a primer ratio of 10:1 for *SMN*202-F/*SMN*202-R. PCR products were quantified using both agarose gel electrophoresis and HPLC with a Waters Gen-Pak FAX anion-exchange column [using 25% Buffer B (25 mM Tris, 1 mM EDTA, 20% acetonitrile 1 M NaCl, pH 8.0)/75% Buffer A (25 mM Tris, 1 mM EDTA, 20% acetonitrile, pH 8.0) to a 100% Buffer B linear gradient, applied over 30 min, at a temperature of 30°C].

Instrumentation used for conducting hybridization assays

Hybridization of labeled DNA to surface immobilized probe oligonucleotides was measured by means of a prototype PC driven epifluorescence scanning instrument that was fabricated in-house for use with the fibre-optic sensors in a TIRF format. Excitation of fluorescence was achieved by use of a solid-state laser (7 mW, λ_{max} = 636 nm) that was passed through a 635 nm Laser Line Interference Filter (Oriel Optics/Gamble Technologies, Mississauga, ON, Canada) and incident upon a dichroic reflector mirror (630 nm cut-off; Omega Optical, Battleboro, VT) oriented at 45° to the incident beam. Laser light reflected from the dichroic mirror was directed into the scanning/focusing optics and coupled into the fibre-optic biosensors. Fluorescence emitted from surface-bound

fluorophores captured by the sensing fibres was collected by the focusing optics and directed back towards the dichroic mirror. Radiation of wavelength greater than 630 nm was transmitted through the dichroic mirror and passed through a broadband interference filter (660–760 nm transmission window; Oriel Optics/Gamble Technologies), and was detected using a photomultiplier tube. Sensors were mounted in a hybridization flowcell with maximum capacity of four sensors, designed with a single flow channel so that all sensors interrogated the same sample solution (~25 µl surrounding each sensor), as shown in Figure 1. The temperature of the hybridization flowcell was controlled using a Peltier thermoelectric cooler (Ferrotec America Inc., Nashua, NH) with PC interface (Oven Industries, Mechanicsburg, PA). The temperature of the hybridization solution was determined by using an IC temperature sensor (Analog Devices, Newark, NJ) embedded in a copper jacket surrounding the hybridization flowcell.

Interfacial thermal denaturation profiles were collected using this instrument by applying a temperature ramp over a range from 25 to 85°C, using a temperature ramp rate of 0.3°C/min to ensure that thermal equilibrium was achieved at the time of each measurement. Target oligonucleotides were prepared as 3 nM solutions in 1× TEN (50 mM Tris–HCl, 10 mM EDTA, 1 M NaCl, pH adjusted to 7.0). Following initial equilibration of the targets, measurements were then made every 5 s for the duration of the ramp.

RESULTS AND DISCUSSION

Control of the chemistry of immobilization (synthetic quality, density and homogeneity of distribution of probe molecules, the free energy of the substrate surface and the extent and distribution of strand–strand versus strand–surface interactions) may be used to tune the analytical figures of merit of the sensors (23–26). Increased strand immobilization density results in organization of the immobilized oligonucleotide films and alteration to the physical chemistry of the interfacial film. Such alterations have been observed to enhance the selectivity of hybridization and can be used to ameliorate the extent of non-selective adsorption and dependence between selectivity and ionic strength. Optical fibres functionalized with covalently immobilized oligonucleotides selective for either *SMN1* or *SMN2* were prepared as described previously (26) at a high oligonucleotide immobilization density (~7 pmol/cm^2).

Figure 2 illustrates a typical thermal denaturation experiment. Data were concurrently collected following equilibration of sensors functionalized with *SMN1* or *SMN2* probes with a solution containing Cy5-labeled target oligonucleotide. The profiles generated showed clear discrimination of single base mismatches, even in low stringency conditions.

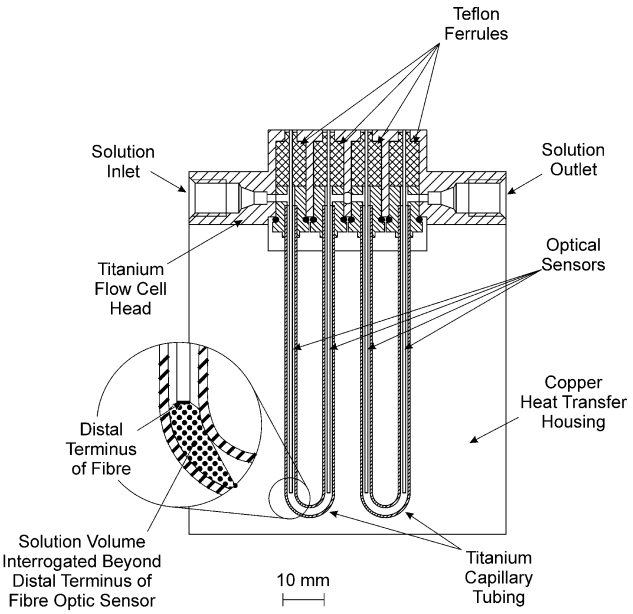

Figure 1. Schematic diagram of the four sensor flow cell. The inset displays the volume of bulk solution interrogated beyond the distal terminus of each optical fibre sensing element.

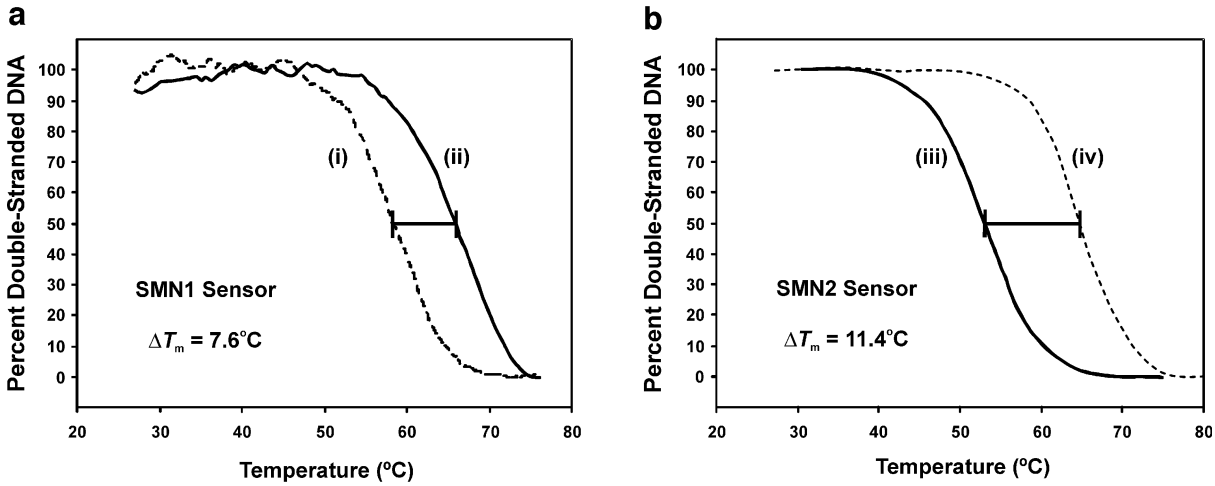

Figure 2. Normalized thermal denaturation profiles of the *SMN1* and *SMN2* sensor constructs. (**a**) Melt temperatures for the *SMN1* probes with *SMN1* target (complement sequence) (i) and *SMN2* target (ii) were determined using 3 nM solutions of each Cy5-labeled target in 1× TEN (1 M NaCl, 50 mM Tris–HCl, 10 mM EDTA, pH 7.0). (**b**) Melt temperatures for the immobilized *SMN2* probes with *SMN1A* (iii) and *SMN2A* (iv) were determined using the procedure stated above.

Importantly, the ability to quantitatively and repeatedly analyze the hybridization characteristics of the sensors provided a means to directly ensure that the T_m values of the *SMN1* and *SMN2* sensors with their respective fully complementary target oligonucleotides were similar (65 ± 1 and 64 ± 1°C, respectively). This permitted simultaneous analysis of samples having varying ranges of *SMN1/SMN2* ratios at a single operating temperature. Significant reductions in T_m (7–11°C) were observed for target sequences containing a single base mismatch, even under low stringency conditions (1 M ionic strength). These data are an improvement compared with those obtained from experiments done in bulk solution, where reductions in T_m as a result of the same mismatch were only 6–8°C (unpublished data; 27).

No loss of selectivity was observed in this system as a result of operating in a high ionic strength environment. The difference in T_m (ΔT_m) between thermal denaturation profiles for fully complementary nucleic acid targets and nucleic acid targets containing a single base pair mismatch remained constant (and in some cases increased) as a result of increasing the buffer ionic strength from 0.1 to 1.0 M. Furthermore, a substantial reduction in susceptibility to non-selective adsorption in high ionic strength buffers was observed for the sensors functionalized with probes at high versus low immobilization density. This maintenance of selectivity in low-stringency conditions is attractive since it results in rapid hybridization kinetics in high ionic strength buffers (28) and permits the complexity of sample preparation methods (i.e. sample dilution or salt elimination) to be substantially minimized.

Taton *et al.* (2) have demonstrated that significant sharpening in the slope of thermal denaturation transitions may be imparted for assays involving the use of oligonucleotides immobilized onto gold nanoparticles and monitoring of hybridization via changes in the chromophoric properties of the nanoparticles induced by DNA-directed aggregate formation. In that work, ~60% retention of the signal for a fully matched 12mer target was demonstrated at the lowest operating temperature where the signal for an oligonucleotide target containing a central mismatch was completely diminished. Our work demonstrates comparable assay selectivity where, as observed in Figure 2b, ~30% retention of a fully matched 19mer target is observed at the lowest operating temperature at which the oligonucleotide target containing a central mismatch completely dissociated. Preliminary investigations of the use of shorter immobilized *SMN1* probes (12 nt in length) have resulted in similar selectivity to that reported by Taton *et al.* in which 60–70% retention of the fully complementary hybrid was maintained at the temperature where complete dissociation of the SNP was observed (ΔT_m of ~14°C in 1.0 M ionic strength buffer, see Fig. 3). Selectivity in this system is derived from suppressed non-selective adsorption, maximal separation of the thermal denaturation profiles and sharpening of the transition as afforded by control of probe immobilization density, homogeneity and linker chemistry. Furthermore, the ΔT_m between the fully matched and single nucleotide mismatched hybrids used by Taton *et al.* was significantly lower than that predicted by use of software algorithms (27) based on the thermodynamic analysis of SantaLucia *et al.* (29). As such, the selectivity of the nanoparticle-based system is derived from the sharpness of the transitions alone; however, it may be offset by the lower than predicted ΔT_m.

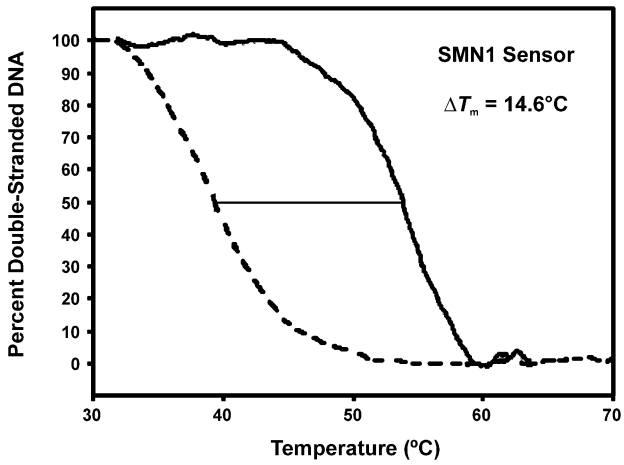

Figure 3. Selectivity of the optical biosensor functionalized with short oligonucleotide probes. Normalized thermal denaturation profiles of a sensor functionalized with *SMN1* probes that were 12 nt in length following hybridization with *SMN1A* and *SMN2A* targets in 1× PBS.

Interestingly, substantially lower T_m values (by ~10°C) for the *SMN1* and *SMN2* fully complementary hybrid systems in bulk solution were predicted relative to those observed in interfacial thermal denaturation experiments done using 3 nM concentrations of target nucleic acid. To our knowledge, others who have directly investigated the thermodynamic properties of immobilized nucleic acids have observed reduced T_ms with respect to those of similar systems of nucleic acids in solution.

In greater detail, the work of Fotin *et al.* (30) demonstrated that short oligonucleotides immobilized onto polyacrylamide pads on a microarray substrate provided substantial (~20°C) decreases in T_m of immobilized hybrids with respect to similar systems in solution (wherein strand concentration effects were taken into consideration). Interestingly, the author's note that working in the gel matrix reduced the difference in T_m between immobilized hybrids with respect to those in solution as compared with other immobilized oligonucleotide systems on solid substrates. To help explain the difference in solution versus immobilized hybrid T_ms, it was suggested that the presence of amide moieties in the polyacrylamide matrix may serve to destabilize the nucleic acids in a similar motif as provided by formamide in the competitive destabilization of nucleobase hydrogen bonding interactions. However, on examining the effect of a comparable amount of formamide introduced to the solution based system, it was determined that the surface destabilization was far greater than that solely based on the presence of amide moieties. Interestingly, the authors also observed that the presence of a polyethylene based linker (similar to that used in this work) between the gel matrix and the terminus of the nucleic acid yielded no alteration to the stability of interfacial hybrids. Peterlinz and Georgiadis (31) investigated interfacial thermodynamics of nucleic acid hybrid formation based on the use of thiol-terminated oligonucleotide probes bound to planar gold substrates. In this investigation, a ~5°C reduction in T_m for interfacial hybrids was observed relative to a calculated value

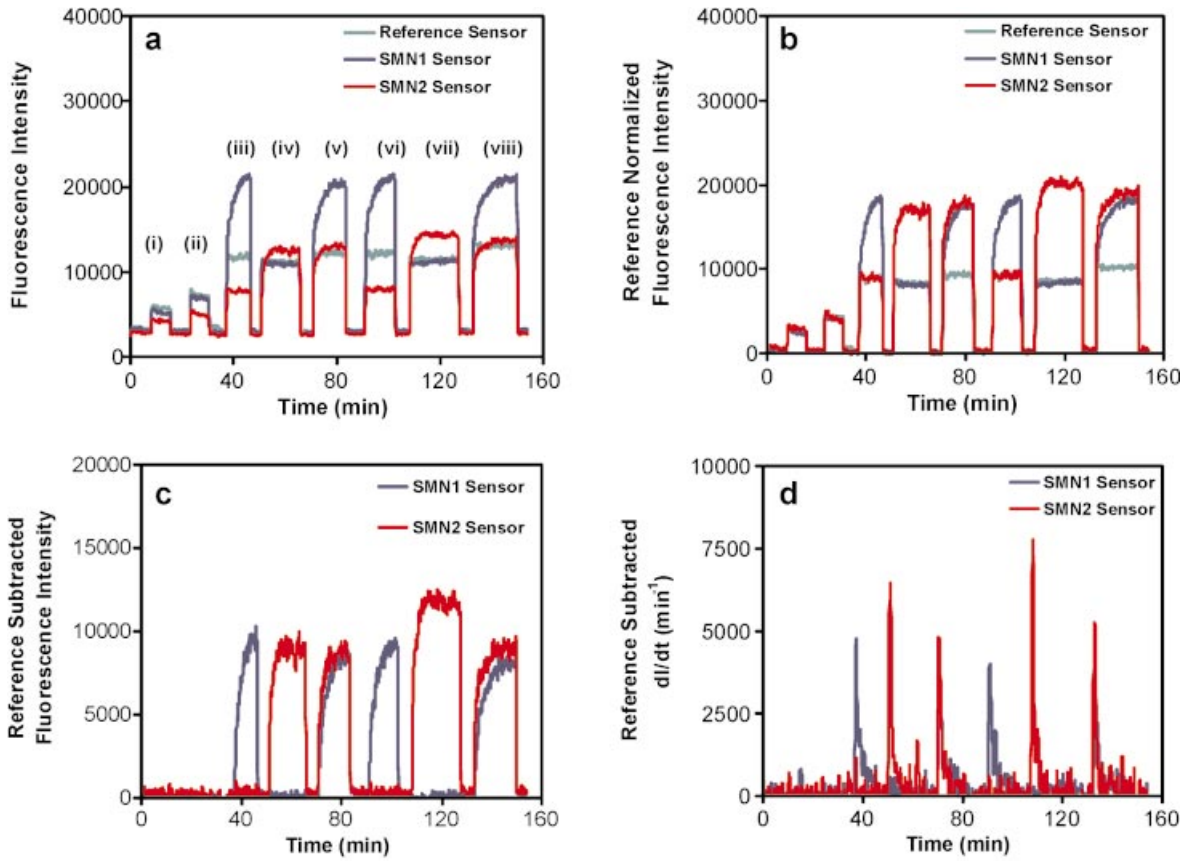

Figure 4. Data processing steps for the optical nucleic acid biosensor. (**a**) Raw fluorescence data corresponding to the exposure of *SMN1*, *SMN2* and reference sensors to solutions of PCR products of different composition; non-complementary DNA serving as a calibrant (i and ii); positive for *SMN1* gene, negative for *SMN2* gene (iii and vi); negative for *SMN1* gene, positive for *SMN2* gene (iv and vii); equal dosage in both *SMN1* and *SMN2* genes (v and viii). Crude PCR mixtures were diluted 1:25 in 1× TEN. (T = 58°C). (**b**) Partial correction of raw data in (a) by normalization of sensor for non-complementary DNA responses to that of the reference sensor. (**c**) Further correction of normalized *SMN1* and *SMN2* sensor responses by subtraction of non-selective signal component. (**d**) Time-derivative of reference-subtracted fluorescence data in (c).

for the similar solution based system of nucleic acids. The validity of this obviously depends on the accuracy of the empirical predictive model that was used.

Persson *et al.* (32) determined that the thermodynamic response characteristics of biotinylated-oligonucleotides immobilized onto streptavidin functionalized hydrogel matrix (on a Sensor chip SA from Biacore) were similar to that predicted using the methods of both Breslauer *et al.* (33) and Doktycz *et al.* (34).

Thiel *et al.* (35) have investigated a device for nucleic acid determinations based on surface plasmon resonance imaging. In this system, a gold substrate was first functionalized with a monolayer of mercaptoundecanoic acid onto which a layer of poly(L-lysine) was electrostatically bound. The film of poly (L-lysine) was then treated with 1,4-phenylenediisothiocyanate to yield an isothiocyanate-derivatized surface, to which 5′-amine-terminated oligonucleotides could then be bound. Substantially reduced T_ms (>10°C) for immobilized oligonucleotides were observed relative to similar oligonucleotide systems in solution; however, this may be due in part to the shift in equilibrium binding resulting from the removal of materials from the system owing to the necessity to wash the sensor prior to imaging detection.

Based on this brief review of other work in this field it would appear that T_ms for interfacial hybrids relative to those of similar systems of nucleic acids in solution may range from being significantly suppressed to similar (i.e. within a few degrees Celsius) in value. In all cases, different immobilization chemistries and substrates were used, suggesting that the nature of the substrate, chemistry used for immobilization and resultant physical chemistry of the interface play a significant role in establishing the resultant thermodynamics of interfacial nucleic acid hybridization and the selectivity of biomolecular interactions. Little work has been done to further elucidate these factors from a thermodynamic standpoint, which sets the foundation for ongoing research work. In the case of the present work, it may be that significantly larger local concentrations exist within the densely packed oligonucleotide films, than that which may be present in bulk solution, contributing to the shift from predicted thermodynamic properties. The T_m values observed in interfacial thermal denaturation experiments were consistent with predicted outcomes for experiments done in solution at two to three orders of magnitude greater nucleic acid concentration. Such interfacial stabilization may be of significant benefit when analyzing double-stranded DNA targets as the competition

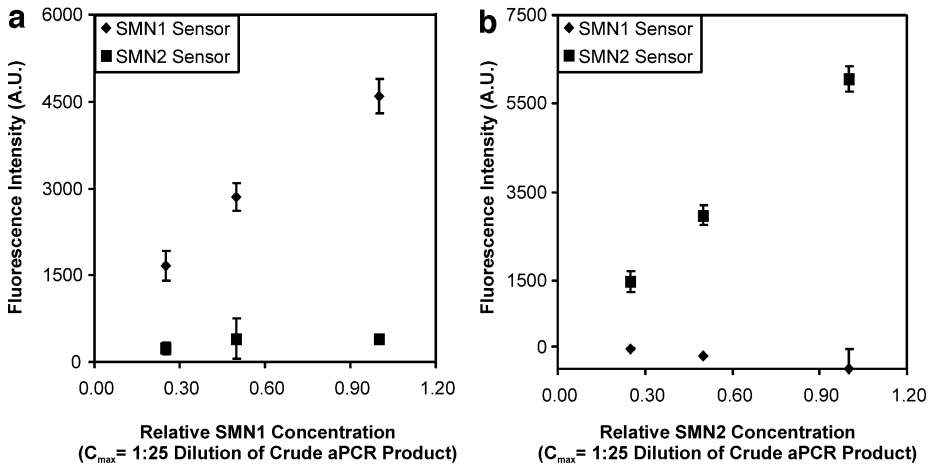

Figure 5. Target concentration dependence of steady-state reference subtracted fluorescence intensities of *SMN1* and *SMN2* sensors. The concentration dependent fluorescence of *SMN1* sensor and *SMN2* sensor was monitored in the presence of PCR products representing either *SMN1* (**a**) or *SMN2* (**b**). In each case, solutions containing PCR amplicons of either single gene dosage in *SMN1* or double gene dosage in *SMN2* were diluted in 1× TEN (T = 58°C) to provide the appropriate concentration.

between formation of interfacial hybrids and re-annealing in solution may be shifted in favor of interfacial hybridization.

Sensors selective for *SMN1* and *SMN2* were used to detect PCR products amplified directly from patient samples having various ratios of these genes (Fig. 4). Quantitative detection with discrimination between sequences differing by a single base pair mismatch was achieved following equilibrium hybridization at 59°C. Most significantly, analysis was done without additional purification and without rinsing to remove non-selectively adsorbed nucleic acids, imparting simplicity and good speed of analysis to this assay method. Previous research has indicated that non-selective adsorptive interactions between nucleic acids in solution and the sensor surface occur independently of selective hybridization events in certain concentration regimes (21,36). Thus, contributions to signal due to non-selective adsorption of labeled materials and fluorescence originating in bulk solution via excitation and recovery from fluorophores located beyond the uncoated distal terminus of the sensors may be determined from the response of the non-selective reference sensor signal following normalization of the sensitivity of the sensors. This non-selective contribution may then be directly subtracted from the response of analytical sensors, as shown in Figure 4. This provides a means for automation of data analysis and a reduction in the requirement for pre-analysis sample purification. These features, coupled with quantitative response and the maintenance of selectivity for discrimination of SNPs in high ionic strength, form the basis of a rapid and reusable sensor construct.

Samples containing only *SMN1*, only *SMN2* or both *SMN1* and *SMN2* target sequences were clearly differentiated by the *SMN1*/*SMN2* sensor system. Replicate analyses (non-consecutive fluorescence measurements) of samples from the same PCR product agreed within 5–15%. Regeneration of sensor surfaces between samples was achieved by use of rinses with deionized water and formamide. The procedure was completed in 5 min, where ~80% of that time was consumed in re-establishment of thermal equilibrium prior to subsequent analysis. Sensors have been reused over the course of many months and many cycles of analysis (approximately 80, unpublished data). It should be noted that the exact figure for the sensor lifetime was difficult to assess as fibre breakage was often the limiting factor. Fibre breakage often occurred on manipulation of the fibre sensors; for example, by removing and reinserting the fibres into the flow cell and also as a result of cold-flow of the Teflon ferrules (see Fig. 1), which often sheared the portion of the fibre secured within the Teflon itself. A more detailed study of the usable lifetime of the sensors is ongoing. The lifetime of 80 cycles represents, roughly, the most usages of a single sensor that were completed prior to failure. Deterioration in sensor performance below a certain threshold in sensitivity or selectivity was not observed or used to provide this indication of reusability. Given that failure of the sensors was catastrophic in nature owing to breakage, the actual lifetime of the sensor is most likely significantly greater than the 80 cycles of application that has been observed to date.

The response of sensors to PCR products of various concentrations was also examined as *SMN1* and *SMN2* copy numbers have been correlated with the SMA phenotype. The *SMN2* copy number has been shown to not vary over a range greater than four (16). Accordingly, the data in Figure 5 show the response of sensors to PCR products derived from samples that carry various quantities of either *SMN1* or *SMN2*. Linear response was observed over the 4-fold concentration range investigated in this work (1:100–1:25 dilution of crude PCR products) with good selectivity of response. A dynamic range of over three orders of magnitude has been demonstrated in other work done using a more advanced prototype instrument (unpublished data). Mixtures of samples containing *SMN1* or *SMN2* were prepared and analyzed in a blinded experiment to determine whether quantitative estimations of the *SMN1*:*SMN2* copy ratio could be made. Quantitative estimates of the *SMN1*:*SMN2* copy ratio that were in agreement with the actual values (Table 2) were observed, suggesting that this technology is suitable for the quantitative evaluation of gene copy numbers routinely observed in a clinical setting.

As can be seen in Figure 4c, sensor response times ranged from ~5 to ~20 min in these experiments. The time course for

Table 2. Results from experiments measuring *SMN1*/*SMN2* content in samples simulating clinical samples for SMA diagnosis

Actual *SMN1* aliquot	Measured *SMN1* aliquot	Actual *SMN2* aliquot	Measured *SMN2* aliquot
0	0.03 ± 0.04 (n = 4)	2	2.4 ± 0.6 (n = 4)
1	1.2 ± 0.2 (n = 3)	3	2.6 ± 0.2 (n = 3)
2	2.6 ± 0.4 (n = 3)	2	2.6 ± 0.3 (n = 3)
3	3.4 ± 0.2 (n = 3)	1	1.2 ± 0.2 (n = 3)

Samples were prepared by mixing crude PCR mixtures that contained either *SMN1* or *SMN2*, in various ratios. Each aliquot was 5 µl into a total final solution of 500 µl.

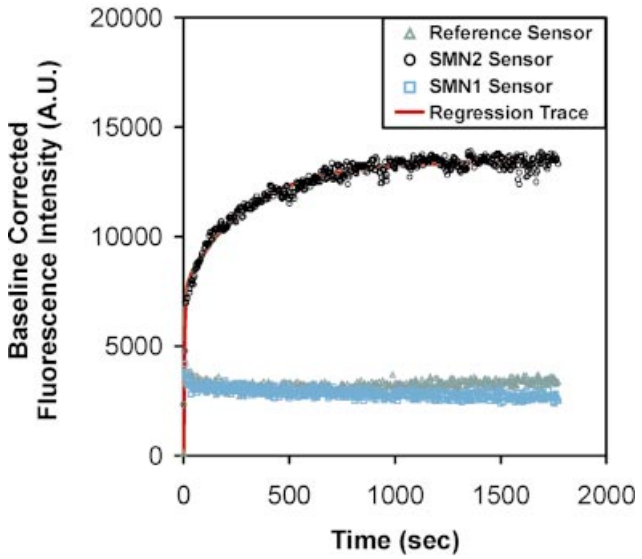

Figure 6. Chronofluorimetric profiles of *SMN1*, *SMN2* and reference sensors. Samples were analyzed following introduction of a solution containing a diluted PCR mixture of *SMN2* amplification product (1:25 dilution in 1× TEN, T = 58°C), along with the curve obtained from regression analysis of the selective binding response.

selective signal evolution, $F(t)$, was evaluated for more than 100 analyses of oligonucleotide and PCR amplicon targets and found to consistently fit to:

$$F(t) = y_0 + a(1 - e^{-bt}) + c(1 - e^{-dt}) \quad \mathbf{1}$$

where y_0, a, b, c and d were parameters determined by nonlinear regression analysis. An example of raw data, along with a best-fit curve according to equation **1**, is shown in Figure 6. Analysis of these data showed that the parameters a and c varied linearly with target concentration while y_0, b and d showed no such correlation. As the experimental temperature was made to approach the T_m of the interfacial hybrid, the values of b and d increased significantly, by up to an order of magnitude (Tables 3 and 4).

These data imply that a significant relationship exists between the rate of fluorescent signal generation and the analysis temperature, relative to the T_m of the sequence of interest, which in turn affects the dehybridization rate constant (37). Equation **1** suggests that quantitative measurements may

Table 3. Summary of statistical parameters for kinetic analysis of oligonucleotide target binding in the concentration range of 0.5–5 nM in 1× TEN at operating temparatures close to interfacial T_m ($T_m - T < 3$°C; n = 10)

Parameter	y_0	a	b	c	d	R^2 (model fit)
Maximum value	1591	7484	0.2485	8396	0.01210	0.981
Minimum value	–64	433	0.0406	1051	0.00194	0.850
Mean	282	3729	0.1537	2837	0.00508	0.920
RSD (%)	175	58	41	77	62	6
Median	72	3798	0.1443	2247	0.00385	0.935

Maximum and minimum values refer to the results of data analysis and do not necessarily correlate with sample concentration for all parameters.

Table 4. Summary of statistical parameters for kinetic analysis of oligonucleotide target binding in the concentration range of 0.5–5 nM in 1× TEN at operating temparatures significantly lower than interfacial T_m (T = 25, 45, 50 and 60°C; n = 35)

Parameter	y_0	a	b	c	d	R^2 (mode1 fit)
Maximum value	23261	21070	0.0585	19390	0.00452	0.998
Minimum value	–1634	561	0.0023	628	0.00050	0.740
Mean	1737	7183	0.0197	6874	0.00198	0.959
RSD (%)	237	85	68	78	50	7
Median	768.5	5434.9	0.0173	6686	0.00170	0.985

Maximum and minimum values refer to the results of data analysis and do not necessarily correlate with sample concentration for all parameters.

be possible prior to the establishment of chemical equilibrium, as shown in Figure 4d. The time derivative of equation **1** may be approximated as:

$$\delta F(t) / \delta t = abe^{-bt} \quad \mathbf{2}$$

for small values of t and when b is substantially larger than d. Given that a was observed to vary with the concentrations observed while b did not, then equation **2** provides a mechanism for measuring sample concentration from plots of time-derivative of fluorescence versus time. As such, quantitative determinations can be made quickly and the sensors may be regenerated for reuse following the achievement of maximum rate of signal increase (~30 s), which occurs well before equilibrium binding and the achievement of full analytical response. Such a strategy may serve to dramatically reduce the analysis time and increase the throughput offered by this sensing technology, where one cycle of application per minute may be achievable (provided that the concomitant improvements in fluid delivery and temperature control hardware could be implemented). Furthermore, the use of such an approach may serve to extend the useful lifetime of the sensors as the extent of surface loading, and hence the amount of washing required for sensor regeneration, should be minimized.

CONCLUSION

The pathophysiology of SMA has been delineated at a gratifying pace over the past decade. With this insight has come the promise of effective therapies for this fatal disorder,

chiefly through the pharmacologic induction of the *SMN2* copy gene. When the diagnosis of SMA is made in an infant or child, a significant proportion of motor neurons have already died. It is clear that the sooner that the diagnosis is made the greater the promise of an effective intervention.

Thus, a rapid diagnostic tool which accurately assesses both *SMN1* and *SMN2* copy number would have tremendous potential for presymptomatic and possibly even prenatal SMA diagnoses. In this regard, SMA is not alone. Cost and labor currently prevent a systematic screening for most genetic diseases at birth. The use of nucleic acid biosensors in a multi-disease configuration for inherited disorders with sufficient mutational homogeneity could allow for early diagnostics for other disorders in addition to SMA.

To this end, this sensor format represents an important step towards the development of biosensors for rapid and quantitative SNP screening. This holds particularly true for the case when the sensitivity of detection is improved through improved optical design, which is the focus of our ongoing research. In addition to speed and selectivity, this technique also represents a highly versatile platform technology for genetic testing with respect to its ability to accommodate samples originating from a broad range of preparation methods. Ultimately this work provides a basis from which development of point-of-care analysis devices may be done.

ACKNOWLEDGEMENTS

Funding for this project was provided in part by FONA Technologies Inc. (a wholly owned subsidiary of Virtek Vision International Inc.), Genome Canada through the Ontario Genomics Institute, the Ontario Ministry of Agriculture and Food through the Healthy Futures for Ontario Agriculture program, the Natural Sciences and Engineering Research Council of Canada and by Agriculture and Agri-Food Canada through the Agricultural Adaptation Council's CanAdapt Program.

REFERENCES

1. Schena,M. (1999) *DNA Microarrays: A Practical Approach.* Oxford University Press, New York, NY.
2. Taton,T.A., Mirkin,C.A. and Letsinger,R.L. (2000) Scanometric DNA array detection with nanoparticle probes. *Science*, **289**, 1757–1760.
3. Yu,C.J., Wan,Y., Yowanto,H., Li,J., Tao,C., James,M.D., Tan,C.L., Blackburn,G.F. and Meade,T.J. (2001) Electronic detection of single-base mismatches in DNA with ferrocene-modified probes. *J. Am. Chem. Soc.*, **123**, 11155–11161.
4. Fan,J.B., Chen,X., Halushka,M.K., Berno,A., Huang,X., Ryder,T., Lipshutz,R.J., Lockhart,D.J. and Chakravarti,A. (2000) Parallel genotyping of human SNPs using generic high-density oligonucleotide Tag arrays. *Genome Res.*, **10**, 853–860.
5. Duggan,D.J., Bittner,M., Chen,Y., Meltzer,P. and Trent,J.M. (1999) Expression profiling using cDNA microarrays. *Nature Genet.*, **21**, 10–14.
6. Hacia,J.G. (1999) Resequencing and mutational analysis using oligonucleotide microarrays. *Nature Genet.*, **21**, 42–47.
7. Lipshutz,R.J., Fodor,S.P.A., Gingeras,T.R. and Lockhart,D.J. (1999) High density synthetic oligonucleotide arrays. *Nature Genet.*, **21**, 20–24.
8. Walker,N.J. (2002) A technique whose time has come. *Science*, **296**, 557–559.
9. Ogino,S. and Wilson,R.B. (2002) Quantification of PCR bias caused by a single nucleotide polymorphism in SMN gene dosage analysis. *J. Mol. Diag.*, **4**, 185–190.
10. Iscove,N.N., Barbara,M., Gu,M., Gibson,M., Modi,C. and Winegarden,N. (2002) Representation is faithfully preserved in global cDNA amplified exponentially from sub-picogram quantities of mRNA. *Nat. Biotechnol.*, **20**, 940–943.
11. Princeet,J.A., Feuk,L., Howell,W.M., Jobs,M., Emahazion,T., Blennow,K. and Brookes,A.J. (2001) Robust and accurate single nucleotide polymorphism genotyping by dynamic allele-specific hybridization (DASH): design criteria and assay validation. *Genome Res.*, **11**, 152–162.
12. Jobs,M., Fredriksson,S., Brookes,A.J. and Landegren,U. (2002) Effect of oligonucleotide truncation on single-nucleotide distinction by solid-phase hybridization. *Anal. Chem.*, **74**, 199–202.
13. Schadt,E.E., Li,C., Ellis,B. and Wong,W.H. (2001) Feature extraction and normalization algorithms for high-density oligonucleotide gene expression array data. *J. Cell. Biochem.*, **37**, 120–125.
14. Krull,U.J., Brown,R.S. and Vandenberg,E.T. (1991) Fiber optic chemoreception. In Wolfbeis,O.S. (ed.), *Fiber Optic Chemical Sensors And Biosensors.* CRC Press, Boca Raton, Vol. II, pp. 315–340.
15. Lefebvre,S., Burlet,P., Liu,Q., Bertrandy,S., Clermont,O., Munnich,A., Dreyfuss,G. and Melki,J. (1997) Correlation between severity and SMN protein level in spinal muscular atrophy. *Nature Genet.*, **16**, 265–269.
16. Burghes,A.H.M. (1997) When is a deletion not a deletion? When it is converted. *Am. J. Hum. Genet.*, **61**, 9–15.
17. Feldkötter,M., Schwarzer,V., Wirth,R., Wienker,T.F. and Wirth,B. (2002) Quantitative analyses of SMN1 and SMN2 based on real-time LightCycler PCR: fast and highly reliable carrier testing and prediction of severity of spinal muscular atrophy. *Am. J. Hum. Genet.*, **70**, 358–368.
18. Lorson,C.L., Hahnen,E., Androphy,E.J. and Wirth,B. (1999) A single nucleotide in the SMN gene regulates splicing and is responsible for spinal muscular atrophy. *Proc. Natl Acad. Sci. USA.*, **96**, 6307–6311.
19. McAndrew,P.E., Parsons,D.W., Simard,L.R., Rochette,C., Ray,P.N., Mendell,J.R., Prior,T.W. and Burghes,A.H. (1997) Identification of proximal spinal muscular atrophy carriers and patients by analysis of SMNT and SMNC gene copy number. *Am. J. Hum. Genet.*, **60**, 1411–1422.
20. Cusco,I.R., Barcelo,M.J., Baiget,M. and Tizzano,E.F. (2002) Implementation of SMA carrier testing in genetic laboratories: comparison of two methods for quantifying the SMN1 gene. *Hum. Mutat.*, **20**, 452–459.
21. Piunno,P.A.E., Watterson,J., Wust,C. and Krull,U.J. (1999) Considerations for the quantitative transduction of hybridization of immobilized DNA. *Anal. Chim. Acta*, **400**, 73–89.
22. Sojka,B., Piunno,P.A.E., Wust,C.C. and Krull,U.J. (1999) Evaluating the quality of oligonucleotides that are immobilized on glass supports for biosensor development. *Anal. Chim. Acta*, **395**, 273–284
23. Shchepinov,M.S., Case-Green,S.C. and Southern,E.M. (1997) Steric factors influencing hybridisation of nucleic acids to oligonucleotide arrays. *Nucleic Acids Res.*, **25**, 1155–1161.
24. Peterson,A.W., Heaton,R.J. and Georgiadis,R.M. (2001) The effect of surface probe density on DNA hybridization. *Nucleic Acids Res.*, **29**, 5163–5168.
25. Oh,S.J., Cho,S.J., Kim,C.O. and Park,J.W. (2002) Characteristics of DNA microarrays fabricated on various aminosilane layers. *Langmuir*, **18**, 1764–1769.
26. Watterson,J., Piunno,P.A.E., Wust,C.C. and Krull,U.J. (2000) Effects of oligonucleotide immobilization density on selectivity of quantitative transduction of hybridization of immobilized DNA. *Langmuir*, **16**, 4984–4992.
27. Su,H., Chong,S. and Thompson,M. (1997) Kinetics of hybridization of interfacial RNA homopolymer studied by thickness-shear mode acoustic wave sensor. *Biosens. Bioelectron.*, **12**, 161–173.
28. Schutz,E. and von Ahsen,N. (1999) Spreadsheet software for thermodynamic melting point prediction of oligonucleotide hybridization with and without mismatches. *Biotechniques*, **27**, 1218–1224.
29. SantaLucia,J.,Jr, Allawi,H.T. and Seneviratne,P.A. (1996) Improved nearest-neighbor parameters for predicting DNA duplex stability. *Biochemistry*, **35**, 3555–3562.
30. Fotin,A.V, Drobyshev,A.L., Proudnikov,D.Y., Perov,A.N. and Mirzabekov,A.D. (1998) Parallel thermodynamic analysis of duplexes on oligodeoxyribonucleotide microchips. *Nucleic Acids Res.*, **26**, 1515–1521.
31. Peterlinz,K.A. and Georgiadis,R.M. (1997) Observation of hybridization and dehybridization of thiol-tethered DNA using two-color surface plasmon resonance spectroscopy. *J. Am. Chem. Soc.*, **119**, 3401–3402.

32. Persson,B., Stenhag,K., Nilsson,K., Larsson,A. and Uhlén,M. (1997) Analysis of oligonucleotide probe affinities using surface plasmon resonance: a means for mutational scanning, *Anal. Biochem.*, **246**, 34–44.
33. Breslauer,J.K., Bloecker,F.R. and Marky,L.A. (1986) Predicting DNA duplex stability from the base sequence. *Proc. Natl Acad. Sci. USA*, **83**, 3746–3750.
34. Doktycz,M.J., Morris,M.D., Dormandy,S.J., Beattie,K.L. and Jacobson,K.B. (1995) Optical melting of 128 octamer DNA duplexes. *J. Biol. Chem.*, **270**, 8439–8445.
35. Thiel,A.J., Frutos,A.G., Jordan,C.E., Corn,R.M. and Smith,L.M. (1997) *In situ* surface plasmon resonance imaging detection of DNA hybridization to oligonucleotide arrays on gold surfaces. *Anal. Chem.*, **69**, 4948–4956.
36. Watterson,J.H., Piunno,P.A.E., Wust,C.C., Raha,S. and Krull,U.J. (2000) Influences of non-selective interactions of nucleic acids on response rates of nucleic acid fiber optic biosensors. *Fr. J. Anal. Chem.*, **369**, 601–608.
37. Dai,H., Meyer,M., Stepaniants,S., Ziman,M. and Stoughton,R. (2002) Use of hybridization kinetics for differentiating specific from non-specific binding to oligonucleotide microarrays. *Nucleic Acids Res.*, **30**, e86.